CENTRO DE INVESTIGACIÓN Y DE ESTUDIOS AVANZADOS
DEL INSTITUTO POLITÉCNICO NACIONAL
UNIDAD MONTERREY

Influencia de interacciones antagónicas mediadas por agentes difusibles en la dinámica espacio-temporal de comunidades bacterianas artificiales en medio sólido

Tesis que presenta

Laura Sánchez Gómez

para obtener el grado de

Doctora en Ciencias

con especialidad en

Ingeniería y Física Biomédicas

Director de la Tesis:

Dr. Moisés Santillán Zerón

Apodaca, Nuevo León — Abril, 2023

CENTRO DE INVESTIGACIÓN Y DE ESTUDIOS AVANZADOS
DEL INSTITUTO POLITÉCNICO NACIONAL
UNIDAD MONTERREY

Influence of antagonistic interactions mediated by diffusible substances on the spatiotemporal dynamics of two-dimensional artificial bacterial communities

Thesis presented by

Laura Sánchez Gómez

submitted for the degree of

Doctor of Philosophy

in

Biomedical Engineering and Physics

Thesis Advisor:

Moisés Santillán Zerón Ph.D.

Apodaca, Nuevo León April, 2023

A Tata y a Pitín,
que aunque ya no están, siempre están...

Acknowledgments

A los Drs. Moisés Santillán, Daniel Sánchez, Bruno Escalante y Jesús Rodríguez por su apoyo, paciecia y guía durante este proceso. Por siempre haber creído en mis capacidades y por haber dispuesto espacios de discusión donde podía expresarme libremente.

A Abraham por impulsarme y darme fuerzas cuando sentía que ya no me quedaban.

A mis amigos por no dejarme caer en la locura.

A mi familia por apoyarme desde la distancia.

Al Cinvestav por darme la oportunidad de realizar mi doctorado y a todas las personas que hicieron parte de este proceso.

A Conacyt por otorgarme la beca para realizar mis estudios.

Variables and Parameters

A	Antagonistic bacteria normalized concentration (dimensionless).
R	Resistant bacteria normalized concentration (dimensionless).
S	Sensitive bacteria normalized concentration (dimensionless).
m	Metabolite concentration (dimensionless).
u	Antagonistic substance concentration (dimensionless).
D_A	Antagonistic bacteria diffusion coefficient (mm^2/min).
D_R	Resistant bacteria diffusion coefficient (mm^2/min).
D_S	Sensitive bacteria diffusion coefficient (mm^2/min).
D_m	Metabolite diffusion coefficient (mm^2/min).
D_u	Antagonistic substance diffusion coefficient (mm^2/min).
$\nabla^2 A$	Antagonistic bacteria Laplacian (dimensionless).
$\nabla^2 R$	Resistant bacteria Laplacian (dimensionless).
$\nabla^2 S$	Sensitive bacteria Laplacian (dimensionless).
$\nabla^2 m$	Metabolite Laplacian (dimensionless).
$\nabla^2 u$	Antagonistic substance Laplacian (dimensionless).
r_A	Antagonistic bacteria intrinsic growth rate $\left(\text{min}^{-1}\right)$.
r_R	Resistant bacteria intrinsic growth rate $\left(\text{min}^{-1}\right)$.
r_S	Sensitive bacteria intrinsic growth rate $\left(\text{min}^{-1}\right)$.

r_m Metabolite intrinsic growth rate $\left(\text{min}^{-1}\right)$.

r_u Antagonistic substance intrinsic growth rate $\left(\text{min}^{-1}\right)$.

K_A Concentration of metabolite needed to reduce r_A down to $r_A(1 - d/2)$ (dimensionless).

K_R Concentration of antagonistic substance needed to reduce r_R down to $r_R(1 - d/2)$ (dimensionless).

K_S Concentration of metabolite needed to reduce r_S down in half (dimensionless).

K_u Half saturation constant of antagonistic substance (dimensionless).

n_A Hill coefficient for antagonistic bacteria (dimensionless).

n_R Hill coefficient for resistant bacteria (dimensionless).

n_S Hill coefficient for sensitive bacteria (dimensionless).

n_u Hill coefficient for antagonistic substance (dimensionless).

d Boundary for Hill equations, it prevents r_A and r_R to reach zero (dimensionless).

α_{AR} Local competition effect of resistant bacteria over antagonistic bacteria (dimensionless).

α_{AS} Local competition effect of sensitive bacteria over antagonistic bacteria (dimensionless).

α_{RA} Local competition effect of antagonistic bacteria over resistant bacteria (dimensionless).

α_{RS} Local competition effect of sensitive bacteria over resistant bacteria (dimensionless).

α_{SA} Local competition effect of antagonistic bacteria over sensitive bacteria (dimensionless).

α_{SR} Local competition effect of resistant bacteria over sensitive bacteria (dimensionless).

γ_m Metabolite decay rate $\left(\text{min}^{-1}\right)$.

γ_u Antagonistic substance decay rate $\left(\text{min}^{-1}\right)$.

Resumen

Se ha demostrado que las interacciones bióticas juegan un papel importante en la formación de comunidades bacterianas. Varios estudios han encontrado que bacterias resistentes ayudan a las cepas sensibles a sobrevivir en presencia de bacterias antagónicas, un fenómeno conocido como facilitación. Los mecanismos responsables aun no han sido identificados, pero la transferencia horizontal de genes parece ser la raíz de varias de estas observaciones. En un trabajo reciente, se encontró evidencia de un mecanismo no genético diferente con un resultado similar. En este proyecto, investigamos la viabilidad de este nuevo mecanismo utilizando un modelo matemático de reacción-difusión. Nuestros hallazgos lo validan, siempre que las bacterias sufran cambios metabólicos drásticos en altas densidades de población. Es importante tener en cuenta que este estudio considera colonias bacterianas bidimensionales que crecen sobre un sustrato sólido, lo que limita la validez de nuestra conclusión a comunidades bacterianas que crecen en condiciones similares.

Abstract

Biotic interactions have been shown to play an important role in the formation of bacterial communities. Various studies have found that resistant bacteria help sensitive strains survive antagonistic bacteria, a phenomenon known as facilitation. The mechanisms responsible have not been clearly identified, but horizontal gene transfer appears to be at the root of several such observations. In a recent work, evidence was found for a different non-genetic mechanism that achieves a similar result. In the current project, we investigate the feasibility of this new mechanism using a reaction-diffusion mathematical model. Our findings validate it, as long as bacteria undergo drastic metabolic changes at high population densities. Take note that the current study considers 2-dimensional bacterial colonies growing on a solid substrate, which limits the validity of our conclusion to bacterial communities growing under similar conditions.

Contents

List of Figures

List of Tables

Introduction

Bacteria have inhabited Earth for billions of years and can be found even in the most inhospitable places (DeLong and Pace, 2001; Horner-Devine et al., 2003). However, their ability to survive almost everywhere is not their only interesting feature. Bacterial interactions are of great importance, allowing the existence of complex communities, where several species can thrive either by competing for or sharing resources (Stubbendieck and Straight, 2016; Qian and Akçay, 2020; Friedman and Gore, 2017). Although these interactions occur at a microscopic range, they can have a huge impact at a much bigger scale (Cordero and Datta, 2016). One reason for this is that bacteria have established strong relationships with every other living organism on Earth, often in the form of parasite-host associations. Diverse communities of bacteria live in and on other life forms, and their niches come in different sizes (Stubbendieck et al., 2016; Currie, 2001). The disturbance of such communities not only affects the community itself, but it can also affect the health of the host. Another reason is that bacterial communities lacking a host also play key roles for life to happen (Stubbendieck et al., 2016; Turnbaugh et al., 2007). They are in charge of processes that can only be performed by them. For instance, the decomposition of dead organisms by bacteria liberates nutrients, and nitrogen fixation converts molecular oxygen in ammonia and other nitrogenous compounds making them available for other life forms (Horner-Devine et al., 2003; Koeppel et al., 2008; Falkowski et al., 2008).

Previous studies of microorganisms focused primarily on physiology and bacterial growth in pure culture, rather than on interactions and community formation (DeLong and Pace, 2001; Zwietering et al., 1990; Pipe and Grimson, 2008; Tittsler and Sandholzer, 1936; Kim and Gadd, 2008). However, interest in the importance of bacterial communities has been increasing recently (Stubbendieck et al., 2016; Turnbaugh et al., 2007; Jeanson et al., 2015; Friedman and Gore, 2017; Horner-Devine et al., 2003; Kennedy and Volz, 1985; Petrof et al., 2013; Qian and Akçay, 2020; Cordero and Datta, 2016). In this area, two main issues arise: 1) what contributes to bacterial biodiversity? (Knope et al., 2020; Czárán et al., 2002; Reichenbach et al., 2007; Cerritos et al., 2010; Stubbendieck et al., 2016; Horner-Devine et al.,

2003; Ratzke et al., 2020), and 2) what promotes the formation of spatial pattern structures within these communities? (Matsushita et al., 1999; Stubbendieck et al., 2016; Mimura et al., 2000; Kerr et al., 2002; Blanchard and Lu, 2015; Hol et al., 2015; Tekwa et al., 2015; Cordero and Datta, 2016; Pipe and Grimson, 2008; Pérez-Gutiérrez et al., 2013; Zapién-Campos et al., 2015) Answering these questions has proven to be a nontrivial task. For instance, interactions can go as far as meters, but at the same time, two non motile bacteria might not ever interact regardless of how close they are to each other (Stubbendieck et al., 2016; Turnbaugh et al., 2007). This means that it is difficult to determine both the extent and the composition of a given community. As a result, abiotic interactions have been far more studied than biotic interactions (Hall et al., 2008; Retter et al., 2021; Kim et al., 2010; Biggs et al., 2011; Rahman et al., 2021; Giovannoni and Vergin, 2012), and studies developed to understand interactions between individuals are mostly performed with lab modified bacteria strains, rather than with wild-type (Frean and Abraham, 2001; Kerr et al., 2002; Kirkup and Riley, 2004). These studies are of great importance as a first approach. However, recent studies performed using wild-type strains have shown that interactions can be much more complex and diverse than those observed with lab modified species (Gallardo-Navarro and Santillán, 2019; Pérez-Gutiérrez et al., 2013).

An example of this is the collection of culturable thermoresistant bacteria isolated by Cerritos et al. (2010) from the Churince lagoon in Cuatro Ciénegas, Mexico. The collection included 78 different strains, collected from several sampling sites within the lagoon, and more than 6000 antagonistic interactions were later scored by Pérez-Gutiérrez et al. (2013). Two important findings were reported. On the one hand, the communities found in the Churince lagoon present a hierarchical food web-like structure, with four different behaviors: 1) top antagonists that antagonize (inhibit the growth and/or kill) but are not antagonized by other bacteria, 2) intermediate antagonists that are both antagonized and antagonize other bacteria, 3) sensitive bacteria that are antagonized but don't antagonize other bacteria, and 4) resistant bacteria that neither antagonize nor are antagonized by any other strain. On the other hand, although the lagoon presents homogeneous and stable physicochemical conditions, communities from different sampling sites separated by tens of meters differ in structure, suggesting that biotic factors such as antagonistic interactions play a role in maintaining spatial heterogeneity among bacterial communities (Stubbendieck et al., 2016). This contradicts the assumption that in microbial ecology, "everything is everywhere, the system selects", meaning that it is the environment the one that determines microbial communities (O'Malley, 2007).

As highly social organisms, bacteria form complex communities characterized by high biodiversity (Stubbendieck et al., 2016). These communities assemble influenced by both abiotic and biotic interactions, *i.e.* the response to environmental stimuli (presence of nutrients, pH, physical space, among others), and to the presence of neighboring cells of the same and of other species, respectively (Stubbendieck et al., 2016; De Vrieze et al., 2017; Venturelli et al., 2018; Oña and Kost, 2022; Pacheco and Segrè, 2019). Given that bacterial communities are almost never of only two species, and studying wild-type bacteria in the lab can be very difficult because of the little knowledge there is on nutrient requirements, to fully understand a species, it is imperative to consider its ecological context Richards et al. (2018); Stubbendieck et al. (2016); Stubbendieck and Straight (2016); Turnbaugh et al. (2007). Moreover, biodiversity is promoted by competition and spatial structure, which is why studying communities and not individual species will provide more information into what mechanisms are involved in complex bacterial dynamics (Cordero and Datta, 2016).

Bacterial communities are not homogeneous (Stubbendieck et al., 2016). Nutrient distribution, pH and temperature gradients, among other things, build micro-environments that locally (in a small vicinity) modify the community (Friedman and Gore, 2017). Micro-environments produce cell aggregates in which distance between cells is short enough so that diffusible metabolites reach neighboring cells (Cordero and Datta, 2016; Stubbendieck et al., 2016). Closeness to one another also promotes competition between individual cells, based on their metabolic and physiological needs (Stubbendieck et al., 2016). These local interactions generate spatial heterogeneity depending on who is next to whom (Friedman and Gore, 2017). Otherwise, in a well-mixed environment one species will outcompete (Cordero and Datta, 2016; Horner-Devine et al., 2003). Nonetheless, this alone does not maintain biodiversity. An example of this is the rock-paper-scissors dynamics described by Kerr et al. (2002), Frean and Abraham (2001) and Reichenbach et al. (2007) that presents cyclic competition. Consider three different bacterial species A, B and C with the following characteristics: A kills B; B outgrows C; and C outgrows A. When processes like dispersal, movement and interactions occur at a small spatial scale, competing species can coexist (Friedman and Gore, 2017; Kerr et al., 2002). However, when they occur at a large spatial scale, *e.g.* mobility exceeds a threshold, coexistence is lost and only one species survives (Reichenbach et al., 2007).

Mathematical modeling has been used as a tool to explore what mechanisms within bacterial interactions allow the formation of such diverse communities (Bomze, 1983; Pipe and Grimson, 2008; Martins and Gjini, 2020; Zapién-Campos et al., 2015; Aguirre-von Wobeser et al., 2015; Kerr et al., 2002; Mimura et al., 2000; Reichenbach et al., 2007). Results ob-

tained by Zapién-Campos et al. (2015) using the antagonism matrix of Pérez-Gutiérrez et al. (2013)via a cellular automaton model, suggest that co-existence of different bacterial species is possible when resistant bacteria impede physical interactions between antagonistic and sensitive strains. Their simulations also showed that such co-existence depends highly on spatial structure. When the effect of flows were simulated by randomly rearranging all bacteria, resistant bacteria were no longer able to protect sensitive strains leading to their death. Nonetheless, experiments performed by Gallardo-Navarro and Santillán (2019) showed that acting as a physical barrier is not the only mechanism that promotes biodiversity. They chose a sensitive, a resistant and an antagonistic strain from the collection isolated from the Churince lagoon by Cerritos et al. (2010). Although they did not observe the latter mechanism, several findings were made: 1) when an antagonistic colony was faced with any other colony (including a colony of the same strain), its growth was slowed, 2) when a colony of resistant bacteria was faced with an antagonistic colony its growth was slowed as well, but this did not happen when faced with a colony of the sensitive strain, 3) when a sensitive colony was faced with an antagonistic colony its growth stopped, however when faced with a resistant colony its growth was not affected, and 4) in the presence of resistant bacteria, sensitive bacteria were more likely to survive antagonism than when they were cultured only with antagonistic bacteria.

The study of bacterial communities is of great importance. It can help us understand how biodiversity and stability are accomplished, what characteristics define these communities well-being, and how disruptions affect both stability and biodiversity (Petrof et al., 2013; Qian and Akçay, 2020). Moreover, it can help us deal with emerging issues like antibiotic resistance. The work of Gallardo-Navarro and Santillán (2019) showed evidence of a mechanism different from the physical barrier described by Pérez-Gutiérrez et al. (2013), participating in the assembly of complex bacterial communities where sensitive bacteria coexist with antagonistic bacteria, and also that this coexistence is favored by resistant bacteria. However, neither their experiments or their mathematical model explicitly describe said mechanism. To explore and contribute to the answers to these and to many other related questions, we developed a mathematical model considering a small community of three different species of bacteria: an antagonistic, a sensitive, and a resistant strain, that we believe is a particular case of the rock-paper-scissors dynamics. We propose that antagonistic bacteria sense neighboring bacteria through either the presence or the increase in the concentration of a metabolic by-product, and they respond by secreting a harmful substance. This antagonistic substance kills sensitive bacteria but is countered by the resistant strain. Our model is a system of PDEs, in order to emphasize the importance of spatial distribution in community assembly and in

maintaining biodiversity. We included local interactions using Lotka-Volterra competitive equations and we used Hill functions to simulate antagonistic interactions. We evaluated the feasibility of the proposed mechanism while discussing three different scenarios. In the first scenario we assume the metabolic by-product is common to all three strains, and an increase in its concentrations triggers the production and release of the antagonistic substance; in scenario number two, we assume the metabolite is only released by the resistant and the sensitive strains and its presence is what triggers a response by antagonistic bacteria; finally, we consider the possibility that when bacteria population reaches a certain density, they modify their metabolism and no longer participate in growth, migration, cell division or metabolite secretion.

Chapter 1

Hypothesis

In small bacterial communities in solid media, antagonistic bacteria sense de proximity of other bacteria via a common metabolite that diffuses in the media. As a response, antagonistic bacteria produce and secrete an antagonistic substance that also diffuses in the media in order to reduce competition, while paying a metabolic cost. Sensitive bacteria are killed and their growth is inhibited by the toxicity of said antagonistic substance, while resistant bacteria are able to counteract its effects, albeit at a metabolic cost. The presence of resistant bacteria induces de production of antagonistic substance affecting the growth of antagonistic bacteria. This indirectly increases the likelihood of sensitive bacteria locally outcompeting antagonistic bacteria. Our hypothesis is that the mechanisms described above are mathematically consistent with experimental observations.

Chapter 2

Objectives

2.1 General Objective

To investigate how antagonistic interactions impact the assemble of small artificial bacterial communities via a mathematical model.

2.2 Specific Objectives

- To study the mechanisms described by Gallardo-Navarro and Santillán (2019) using a mathematical tool in an artificial community of resistant-antagonistic-sensitive bacteria in a two-dimensional environment.
- To study the role of competition and antagonistic interactions mediated by diffusible substances in shaping the structure of small artificial bacterial communities.

Chapter 3

Methodology

Gallardo-Navarro and Santillán (2019) reported that the presence of resistant bacteria helps sensitive bacteria to survive when they are present in an artificial community of wild-type bacteria that included antagonistic, sensitive, and resistant strains. They also proposed the following mechanism of interaction between the three strains: Antagonistic bacteria sense the presence of other bacteria via a common metabolite that diffuses in the medium, and in response they produce an antagonistic substance with the concomitant metabolic cost. The toxicity of the antagonistic substance inhibits the growth and kills sensitive bacteria, whilst resistant bacteria are able to counteract its effect at the expense of a metabolic cost. We developed a mathematical model to test the mechanism.

3.1 Mathematical Model Development

The following mathematical model uses reaction-diffusion equations to study the spatio-temporal dynamics of three different bacterial strain populations: one antagonist (A), one resistant (R) and one sensitive (S). Our model also accounts for the dynamics of a common metabolite (m), product of bacterial metabolism, and an antagonistic substance (u), produced by the antagonist strain:

$$\frac{\partial A}{\partial t} = D_A \nabla^2 A + r_A \left(d \frac{K_A^{n_A}}{K_A^{n_A} + m^{n_A}} + (1-d) \right) (1 - A - \alpha_{AR} R - \alpha_{AS} S) A, \tag{3.1}$$

$$\frac{\partial R}{\partial t} = D_R \nabla^2 R + r_R \left(d \frac{K_R^{n_R}}{K_R^{n_R} + u^{n_R}} + (1-d) \right) (1 - R - \alpha_{RA} A - \alpha_{RS} S) R, \tag{3.2}$$

$$\frac{\partial S}{\partial t} = D_S \nabla^2 S + r_S \left(\frac{K_S^{n_S}}{K_S^{n_S} + u^{n_S}} \right) (1 - S - \alpha_{SA} A - \alpha_{SR} R) S, \tag{3.3}$$

$$\frac{\partial m}{\partial t} = D_m \nabla^2 m + r_m (A + S + R) - \gamma_m m, \tag{3.4}$$

$$\frac{\partial u}{\partial t} = D_u \nabla^2 u + r_u \left(\frac{m^{n_u}}{K_u^{n_u} + m^{n_u}} \right) A - \gamma_u u. \tag{3.5}$$

All model equations indicate the concentration of the species in a determined point in space and a specific moment of time, normalized to the corresponding carrying capacity of the system in the case of bacterial species. The first term in the right hand side is the diffusion term and D_i is the corresponding diffusion coefficient, with $i = A, R, S, m$ or u indicating the species it belongs to. The following term(s) indicate the species growth (or production) and death (or decay) rates, where r_i is the growth/production rate for $i = A, R, S, m$ or u; and γ_m, γ_u are the decay rates for the metabolite and the antagonistic substances, respectively. In this model, local bacterial interactions are simulated via Lotka-Volterra competition equations, where α_{ij} indicates the effect of species j over species i for $i, j = A, R$ or S.

Equation (3.1) models the dynamics of the antagonist strain (A), whose growth rate (r_A) is regulated by a decreasing Hill-like function of the concentration of metabolite (m). This reduction stands for the metabolic cost associated to the synthesis and release of the antagonistic substance, in response to the presence of m. Notice the growth rate reduction is bounded by parameter d. This means that the growth of the antagonist strain is not totally stopped when it synthesizes the antagonistic substance as observed by Gallardo-Navarro and Santillán (2019). K_A is the concentration of m needed to reduce r_A down to $r_A(1 - d/2)$, and n_A is a Hill coefficient.

Equation (3.2) corresponds to the dynamics of the resistant strain (R). Its growth rate (r_R) is also regulated by a decreasing Hill-like function of the antagonistic substance (u). This represents the ability of R to resist u which comes with a metabolic cost as well. K_R accounts for the concentration of u needed to reduce r_R down to $r_R(1 - d/2)$, and n_R is a Hill coefficient. Analogous to the case of A, the presence of u is not enough to stop R's growth completely (Gallardo-Navarro and Santillán, 2019), hence the presence of parameter d.

Equation (3.3) represents the dynamics of the sensitive strain (S). Its growth rate (r_S) is regulated by a decreasing Hill function of the antagonistic substance (u). Given that u kills and prevents S from growing, the strain growth rate can become zero (Gallardo-Navarro and Santillán, 2019). K_S is the concentration of u needed to reduce r_S in half, and n_S is a Hill coefficient.

Equation (3.4) stands for the dynamics of the metabolite (m). Metabolite production (r_m) is proportional to the total bacterial concentration, considering all strains; whereas decay is assumed exponential, with constant rate γ_m.

Finally, equation (3.5) denotes the dynamics of the antagonistic substance (u). An increase in the local concentration of m initiates the production of u, which is represented by an increasing Hill function of m with maximum rate r_u. K_u is the half saturation constant and n_u is a Hill coefficient. As in m, decay for u is assumed exponential, with constant rate γ_u.

3.2 Numerical Solution of the model PDE system

We implemented the finite element method to numerically solve the model PDEs system. In particular, we considered rectangular or square flat areas corresponding to the surface on which bacterial populations grow. In the case in which we use the model to simulate Petri dish experiments, the modeled surface corresponds to a section of the agar surface that is sufficiently far away from the dish walls.

We constructed a mesh with square sub-domains within the simulated surface. To numerically solve model equations in such meshes, we discretized the Laplacian using a fourth order 9-point stencil as described in (LeVeque, 2007). Given that the simulated areas are assumed to be far away from the walls of the dish, we used Dirichlet boundary conditions. This led us to calculate the Laplacian considering three different types of sub-domains provided their location on the grid and the number of adjacent compartments: interior, edges or vertices. The following equations were used to compute the Laplacian on interior, left side edge, and upper-left vertex compartments of the mesh, respectively. Analogous equations were used to calculate the Laplacian in compartments located in the right, upper and lower sides edges and for compartments in the upper-right, lower-left and lower-right vertices of the mesh.

$$\begin{aligned}
\nabla^2 F_{i,j} &= \frac{1}{6\Delta x^2}[4F_{i-1,j} + 4F_{i+1,j} + 4F_{i,j-1} + 4F_{i,j+1} \\
&+ F_{i-1,j-1} + F_{i-1,j+1} + F_{i+1,j-1} + F_{i+1,j+1} - 20F_{ij}], \\
\nabla^2 F_{i,j} &\approx \frac{1}{6\Delta x^2}[4F_{i-1,j} + 4F_{i+1,j} + 4F_{i,j+1} + F_{i-1,j+1} + F_{i+1,j+1} - 20F_{ij}], \\
\nabla^2 F_{i,j} &\approx \frac{1}{6\Delta x^2}[4F_{i+1,j} + 4F_{i,j+1} + F_{i+1,j+1} - 20F_{ij}].
\end{aligned}$$

In the previous equations, $F_{i,j}$ represents the average value of function F in the compartment with coordinates i, j, $\nabla^2 F_{i,j}$ denotes the Laplacian of F in the same compartment, and Δx represents the length of the mesh-compartment side. Its value was set to ($\Delta x \approx 0.1\,\mathrm{mm}$) was chosen by empirically testing the numerical convergence of the algorithm.

Taking into account the above considerations we implemented Euler's algorithm in `Python` to solve the model of PDEs in the discretized surface. The time period corresponding to one algorithm iteration ($\Delta t = 0.01$ or $0.005\,\mathrm{min}$) was also chosen by empirically testing the algorithm numerical convergence. All simulations were repeated five independent times, and mean and standard deviation were calculated. Pseudo code is as following:

1. Set initial values for A, S and R; m and u are initialized with zero in all compartments of the mesh.

2. Calculate the Laplacian of each variable in every compartment of the lattice. The resulting value, when multiplied by the corresponding diffusion coefficient and the time step Δt, determines the change of the variable in each compartment due to diffusion in one iteration.

3. Compute the production and/or degradation of all model variables in each lattice compartment based on the differential-equation terms. These values multiplied by Δt represent the quantity of each variable that is added or removed in each compartment due to the reaction terms of the equations in one iteration.

4. Update the values of all variables by taking into account the changes caused by the reaction and diffusion terms of their respective equations.

5. Iterate to step two.

The Python code is available for interested readers in the repository located at `https://github.com/lsanchezg89/facilitationbacterialcommunity.git`.

Model parameter values were estimated by solving the inverse problem, using experiments performed by Gallardo-Navarro and Santillán (2019). In order to reduce the number of free parameters, we broke down the model into simpler equations resembling their experiments.

3.3 Intrinsic growth rate estimation

To estimate the intrinsic growth rate we used data obtained by Gallardo-Navarro and Santillán (2019) where they estimated bacterial concentration from optical densities as a function of time from experiments of bacteria growing in marine liquid medium. We normalized the reported data to the highest concentration of each bacterial strain, and then we fitted the results to the following logistic function normalized to the corresponding carrying capacity by means of algorithm `curve_fit` implemented in `Python`'s library `SciPy.Optimize`:

$$x = \left(1 + \left(\frac{1}{x_0} - 1\right) e^{-rt}\right)^{-1}. \tag{3.6}$$

The best-fitting r value can be interpreted as the intrinsic growth rate of the corresponding bacterial strain.

3.4 Single colony simulations

We simulated experiments performed by Gallardo-Navarro and Santillán (2019) in which single colonies were inoculated in Petri dishes with marine medium plus 2% agar, and their radii were monitored over a period of 6 days. The area of the Petri dish in which the colonies grow was simulated with a 45 compartments length square grid. Initial bacteria concentration was chosen randomly from a normal distribution with mean of 0.2 and standard deviation of 0.02 for each compartment within a circle-like area of 4 compartment-long radius, and zero elsewhere (see Fig. 3.1A). The initial values of the variables corresponding to the concentrations of other bacterial populations and metabolites m and u were set to zero everywhere. As mentioned in section 3.2, we chose Dirichlet boundary conditions, provided that the simulated area is far away from the walls of the dish. We recorded data at the end of each simulated minute for 6 days.

To measure the radius of each colony, we first used a filter to eliminate concentrations of all bacterial strains bellow 0.01, and counted the number of compartments along the radius that contained bacteria for each simulated minute. As a result of the discretization described in section 3.2, we obtained step-like functions of time (see Fig. 3.1B). To smoothen them

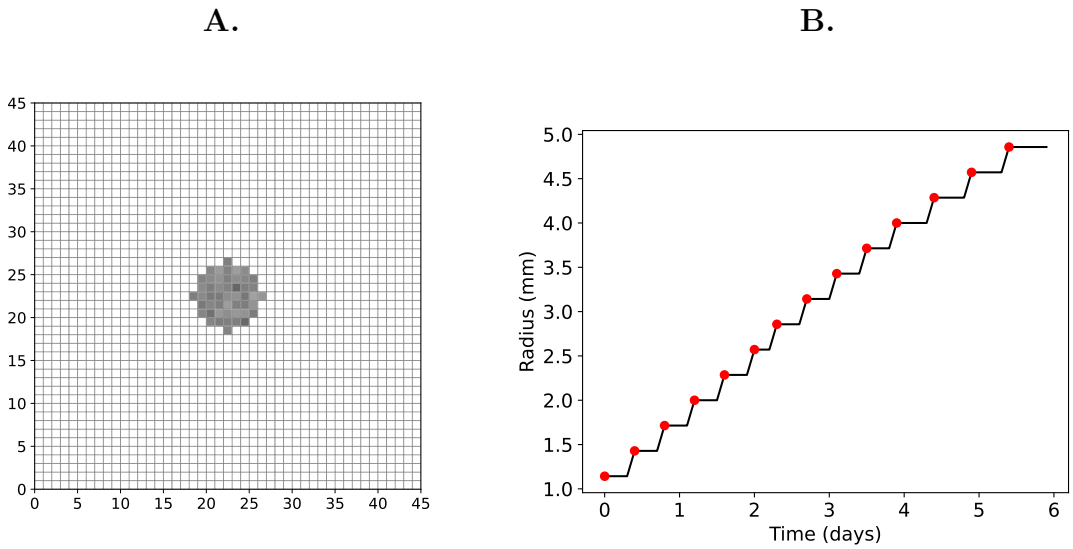

Figure 3.1: **A.** Illustration of initial-condition selection for single-colony simulations. **B.** Illustration of the radius measurement results in single-colony simulations (solid line). Stair vertices used for interpolation are emphasized (solid red points).

we took the vertices of the steps and completed the missing values by means of algorithm `interp1d` from `Python`'s library `SciPy.Interpolate`. All simulations were performed five times and average and standard deviation were calculated.

3.5 Confronted colonies simulations

To study neighboring-colony dynamics under our hypothesis, we simulated the experiments where two bacterial-culture drops of 1 µL each, were inoculated with a separation of 15 mm in a Petri dish with marine medium plus 2% agar. Over a period of 6 days, the external (in the direction opposite to the other colony) and internal (in the direction of the other colony) radii were measured periodically, and the differences between them were calculated.

In the simulations, the surface of the Petri dish was represented with a rectangular grid of 90×144 compartments. Each drop was simulated as a circle-like area of 4 compartment-long radius and the separation between them was of 53 compartments. Initial bacteria concentration was chosen randomly for each compartment within the circle-like area from a normal distribution with mean of 0.2 and standard deviation of 0.02. Bacterial concentration in all compartments outside the circle-like area were set to zero. The initial values of the variables corresponding to the concentrations of other bacterial populations and metabolites m and u were set to zero everywhere. Once again, Dirichlet boundary conditions were chosen and

data was recorded for each simulated minute over a period of time equivalent to 10 days. We measured the external and internal radii of each colony (see Fig. 3.2) in the same way as described in section 3.4.

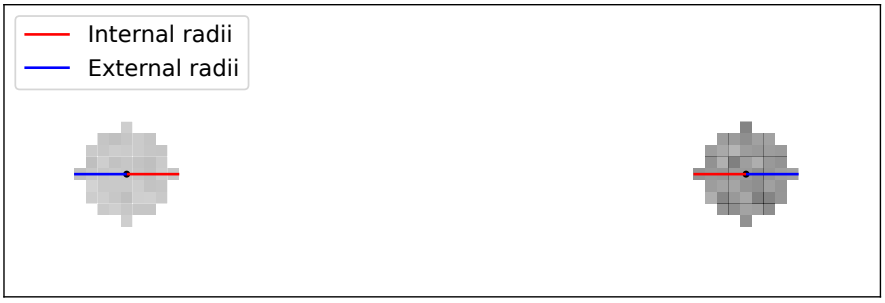

Figure 3.2: Illustration of the initial-condition selection, and of the internal and external radii measurement, for confronted-colonies simulations.

Metabolite and antagonistic substance concentration profiles were obtained by recording the concentration (either m or u) at the end of each simulated day along the row of the mesh where the external and internal radii lie. All simulations were performed five times and average and standard deviation were calculated.

3.6 Artificial communities simulations

To study the dynamics within an artificially created bacterial community under our hypothesis, we simulated the two experiments conducted by Gallardo-Navarro and Santillán (2019). The first experiment consisted in bacterial communities artificially created by mixing a fixed amount of sensitive bacteria with different amounts of antagonists, 10, 25, 50, 75, 100 and 200 % of the initial concentration of sensitive bacteria. 5 µL of the mixture were inoculated in a Petri dish with marine medium plus 2% agar, and incubated for 4 days. The second one consisted in adding to the mixture previously described a fixed amount (500 %) of resistant bacteria. For both experiments the final area-fraction occupied by S was determined as a function of the initial antagonist concentration.

For the simulations, the area of the petri dish in which bacterial population grows was represented with a 60 compartment length square grid. Initial sensitive bacteria concentration was chosen randomly for each compartment of the grid from a normal distribution with mean of 0.2 and standard deviation of 0.02. Initial antagonistic bacteria concentration was chosen randomly from a normal distribution with mean value varying as in the experiments,

and standard deviation of 10% of its value for each compartment of the grid. Once again simulations used Dirichlet boundary conditions. For the second set of simulations, initial resistant bacteria concentration in each compartment was also chosen from a normal distribution with mean of 1.0 and standard deviation of 0.1. We determined the number of compartments occupied by S, and divided by the total number of compartments at the end of each simulated day and up to 20 days. All simulations were performed five times and average and standard deviation were calculated.

Chapter 4

Results and Discussion

Gallardo-Navarro and Santillán (2019) performed experiments with an artificial community of wild-type bacteria (an antagonistic, a sensitive, and a resistant strain) and found that the presence of resistant bacteria aids the sensitive ones in surviving. They also demonstrated that the previously proposed mechanism of resistant bacteria spatially isolating the sensitive from the antagonistic ones does not work for the strains they worked with, and instead proposed the following:

- By sensing an increase in the concentration of a common metabolite that diffuses in the medium, antagonistic bacteria detect the presence of other bacteria.
- In response, antagonists begin the production and secretion of an antagonistic substance in order to reduce competition, at the expense of metabolic cost.
- This antagonistic substance kills as well as inhibits the growth of sensitive bacteria.
- Resistant bacteria can counteract the effect of the antagonistic substance, albeit at a metabolic cost.
- Resistant bacteria slow the growth of antagonistic bacteria by inciting them to produce more antagonistic substance. This indirectly benefits sensitive bacteria.

Gallardo-Navarro and Santillán (2019) provided some indirect evidence to support their proposed mechanisms, but it was insufficient. In this work, we have developed a reaction-diffusion PDE model that incorporates all of the interactions proposed by Gallardo-Navarro and Santillán (2019) with two objectives in mind. On the one hand, we seek to establish whether the aforementioned mechanisms are sufficient to explain the observed behavior or

whether modifications are required. On the other hand, we want to investigate further implications for population dynamics that may arise from such mechanisms.

In order to accomplish the first goal, we looked for parameter values that would allow the model to reproduce, one by one, the various experimental sets from Gallardo-Navarro and Santillán (2019). One benefit of working step-by-step is that we can deal with fewer parameters at once because in each case we can use a reduced model version. Nevertheless, we discovered that the current is a nontrivial multi-objective optimization problem, in the sense that no one parameter setting enables the model to fit all of the experiments. Hence, in order to obtain a reasonable fit to the various experimental data sets, we ultimately fine-tuned all parameter values, which explains why the accuracy of individual fits may not be very good.

Parameter	$\boldsymbol{A}$	$\boldsymbol{R}$	$\boldsymbol{S}$	$\boldsymbol{m}$	$\boldsymbol{u}$
$\boldsymbol{D}\,(\mathrm{mm}^2/\mathrm{min})$	1.7×10^{-7}	5.1×10^{-8}	1.02×10^{-7}	0.34	0.1615
$\boldsymbol{r}\,(\mathrm{min}^{-1})$	0.0078	0.0047	0.0086	0.2	0.2
$\boldsymbol{K}$	1.0×10^{-8}	1.0×10^{-28}	1.0×10^{-14}	NA	1.0×10^{-12}
$\boldsymbol{n}$	3.5	3.0	3.5	NA	3.5
$\boldsymbol{\gamma}\,(\mathrm{min}^{-1})$	NA	NA	NA	0.01	0.01
$\boldsymbol{d}$	0.25	0.25	NA	NA	NA

Table 4.1: Model parameter values for single-colony and confronted-colonies simulations.

We began by fitting the time evolution of normalized populations of bacterial growth from experiments performed by Gallardo-Navarro and Santillán (2019) for the three bacterial strains (antagonistic, sensitive and resistant) in liquid medium, to the logistic model. Representative growth plots for each strain are presented in Figs. 4.1A-C. These fits allowed us to determine growth rate constants for all of the strains (r_A, r_S and r_R) tabulated in Table 4.1. Notice that both the antagonistic and sensitive strains present a much higher growth rate than the resistant strain, consistent with prior observations (Gallardo-Navarro and Santillán, 2019).

We later simulated single colony experiments on solid medium performed by Gallardo-Navarro and Santillán (2019). Using the growth rates previously calculated, we empirically estimated diffusion coefficients for each of the bacterial strains (D_A, D_R and D_S) to fit the

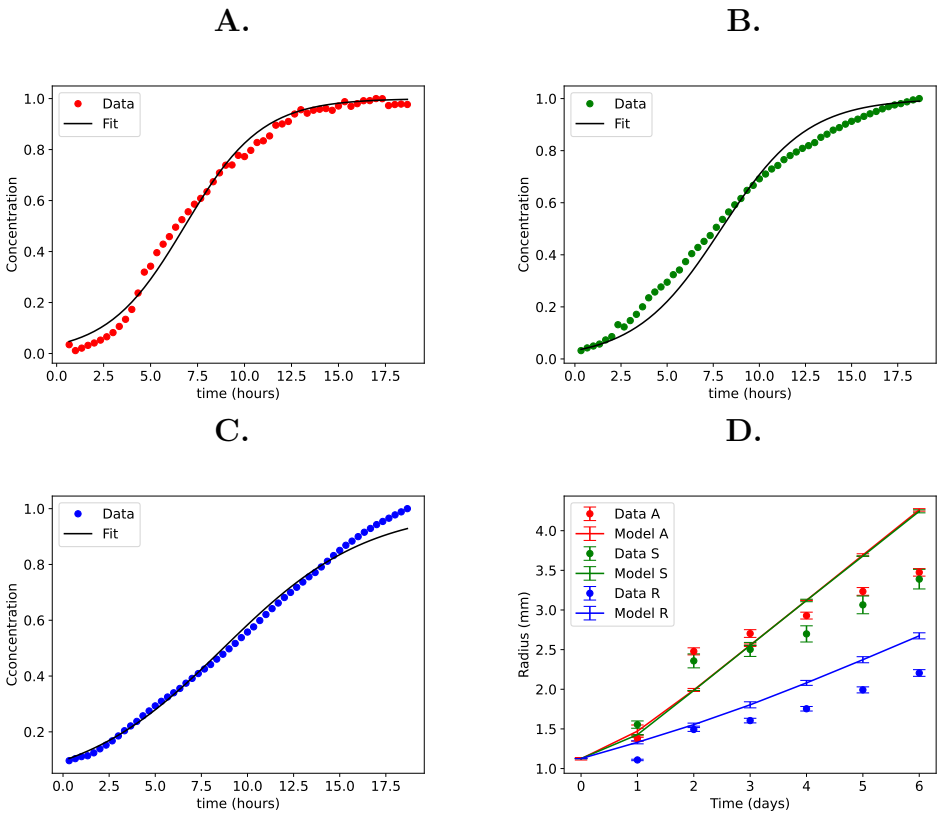

Figure 4.1: Experimental growth curves (Gallardo-Navarro and Santillán, 2019) and best fit to logistic-model equations for the antagonistic (**A.**), sensitive (**B.**) and resistant (**C.**) strains. **D.** Comparison of the simulations of single colonies growing on agar (solid lines) and the corresponding reported experimental results (points). Error bars indicate standard deviation.

reported time evolution of the colony radii. Values are recorded in Table 4.1. Both antagonistic and sensitive bacteria show a higher diffusion coefficient than resistant bacteria, which we attributed to the fact that the sensitive and antagonistic strains chosen by Gallardo-Navarro and Santillán (2019) were motile strains, whilst the resistant was not. Notice that our model is only able to recover qualitatively the experimentally observed bacterial growth rather than quantitatively (See Fig. 4.1D).We think that this is because on the one hand, in contrast to Brownian movement, bacterial movement on agar plates corresponds to swarming (Harshey, 1994, 2003; Daniels et al., 2004; McCarter, 2004; Zorzano et al., 2005). Therefore, modeling it using traditional diffusion is not the most accurate approach. On the other hand, it might be that at the beginning, bacteria present a higher intrinsic growth rate due to a low population density, and as the population density increases, there is a decrease of the intrinsic growth rate as a means to maintain the colony fitness (Smith et al., 2014; Kaul et al., 2016; Goswami et al., 2017; Dressler et al., 2019; Pires et al., 2022). Despite this drawback, we believe that the results obtained are sufficiently accurate for the goals of the current study.

We further simulated experiments of confronting two antagonistic colonies, an antagonist and a resistant, and an antagonist and a sensitive colony (Gallardo-Navarro and Santillán, 2019). It is worth mentioning that we did not perform simulations where two sensitive colonies, two resistant colonies, or a resistant and a sensitive colony were faced. The reason for this was that since neither the sensitive nor the resistant strain produce substance u, their growth would not be affected in either situation, which is consistent with experimental observations (Gallardo-Navarro and Santillán, 2019). We used the previously obtained growth rates and diffusion coefficients, and solved the differential equations as described in section 3.2. We estimated the diffusion coefficient of the antagonistic substance (D_u) using reported diffusion coefficients of chemoattractants in agar (Ahmed et al., 2010; Diao et al., 2006; Cheng et al., 2007) (see Table 4.1). Given that all bacterial strains chosen by Gallardo-Navarro and Santillán (2019) were aerobic, we chose a slightly higher value for D_m, considering carbon dioxide as a potential common metabolite (see Table 4.1). All Hill and Hill-like function parameters in Eqns. 3.1 to 3.5, *e.g.* K_A, K_R, K_S, K_u, n_A, n_R, n_S, n_u, and d, were taken as free parameters and were empirically estimated to fit data reported by Gallardo-Navarro and Santillán (2019). Values for r_m and r_u, were chosen equal for simplicity, as well as γ_m and γ_u. For each simulated situation we measured the external and internal radii over time (see section 3.5). Figs. 4.2A-C show de differences between both radii for each colony as a function of time. The resulting parameter values are listed in Table 4.1.

Both A vs R and A vs S qualitatively recover the experimentally observed differences between external and internal radii of the resistant and the sensitive colony, Figs. 4.2B and C, respectively. This means that near the antagonistic colony, both resistant an sensitive bacteria grow slower, albeit for different reasons. While sensitive bacteria die or stop growing as a result of the toxicity of the antagonistic substance, resistant bacteria reduce their growth rate due to the cost of resisting the antagonistic substance. Experimental data however suggests that these differences do not grow indefinitely unlike what our simulations show. This might be related to the fact that the model was not able to reproduce the two-phase growth in the single colony experiments and keeps a somewhat steady growth. K_R, K_S and K_u in Table 4.1 have very small values to induce an early response of the mechanisms, which means that Hill and Hill-like functions reach the saturation point faster as the edges of the colonies are closer together and reach areas where there is higher concentration of either u or m.

Observe that our model was unable to obtain any differences between external and internal growth in the antagonistic colony for either of the three simulated experiments, that is, it

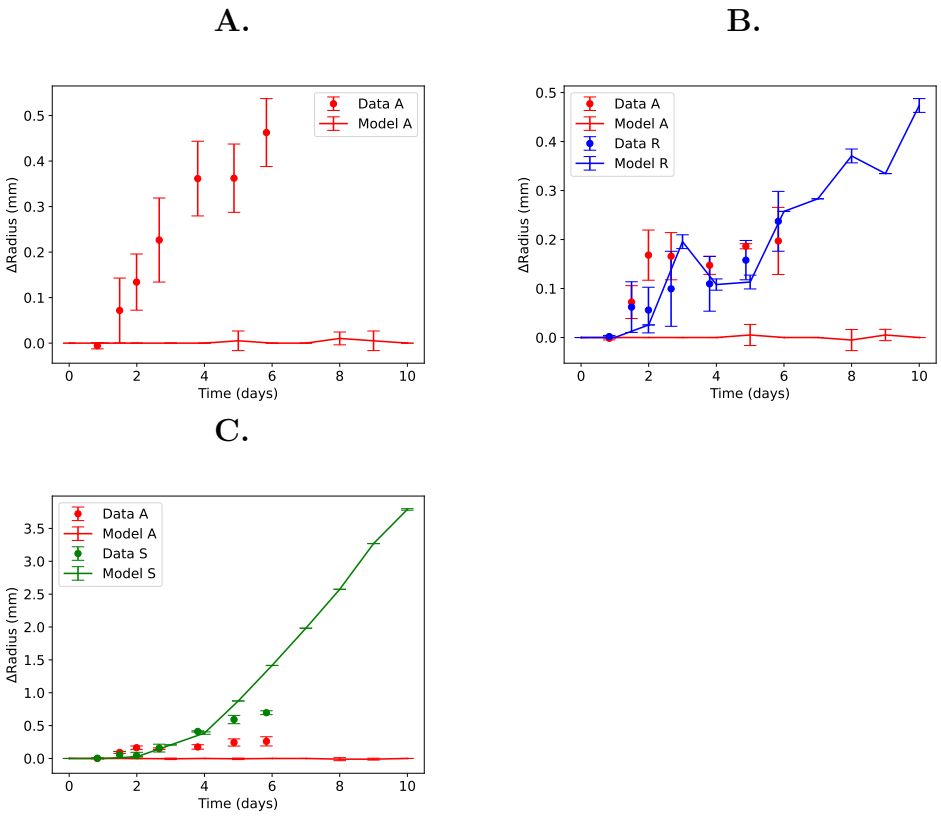

Figure 4.2: Comparison of the simulations of confronted-colonies experiments with the reported experimental results, A vs A (**A.**), A vs R (**B.**) and A vs S (**C.**). ΔRadius is defined as the difference between the external and internal radii of the colony. Error bars indicate standard deviation.

was unable to reproduce the metabolic cost of producing substance u. This occurs because, according to the model, antagonistic bacteria on the periphery of a given colony not only react to the metabolite from bacteria in a nearby colony, but also to that from bacteria within the same colony. As we observed the metabolite concentration profiles (Figs. 4.3A-C), we realized that regardless of the values chosen for the parameters involved, between the two colonies, m was always lower than m in the center of the colony. This could mean that either the threshold is too high that the mechanism never turns on; or that the mechanism of production and release of the antagonistic substance turns on in every cell of the colony rather than only in cells closer to the other colony. Moreover, once the threshold is exceeded, the mechanism stays on indefinitely in cells located in the center of the colony where there is higher bacterial density (see Figs. 4.4A-C).

We tried several parameter combinations but, because of the above described phenomenon, we could not get a significant difference in the concentration of m in the internal and external radii of antagonistic colonies; which is required for differentiated production of the antago-

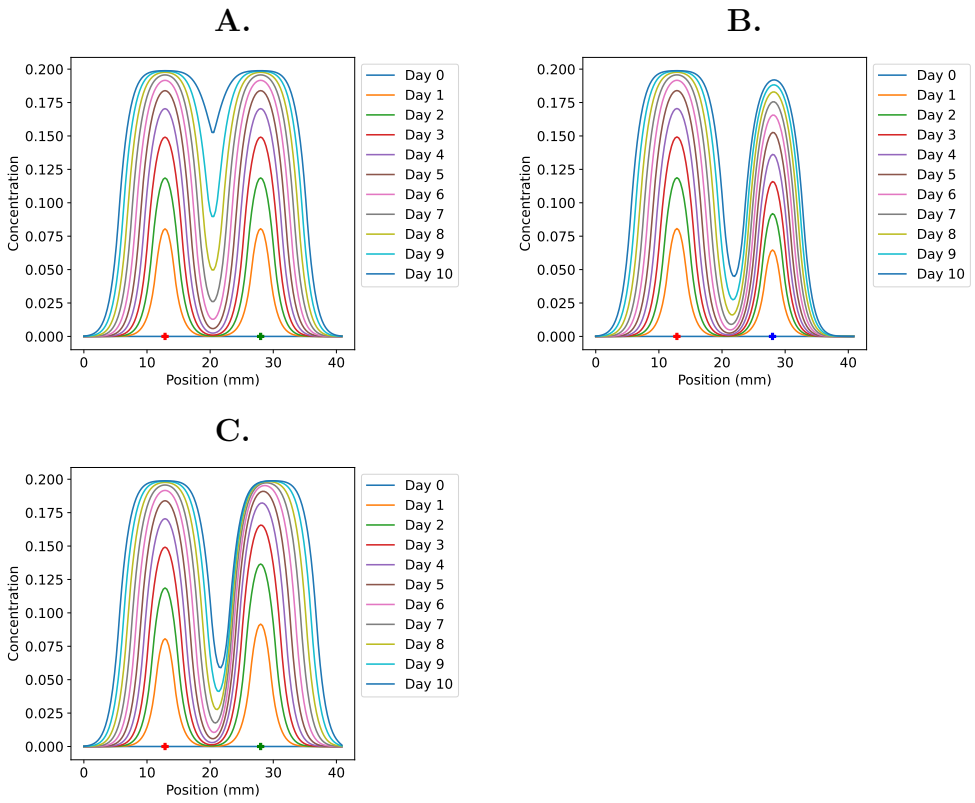

Figure 4.3: Metabolite m profile concentrations for confronted-colonies simulations, A vs A (**A.**), A vs R (**B.**) and A vs S (**C.**). Crosses along the x-axis indicate the center of the colony and the color indicates the strain it belongs to (antagonistic red, resistant blue and sensitive green).

nistic substance and concomitant growth rate affectation. The shortcoming mentioned above led us to conclude that the mechanisms proposed by Gallardo-Navarro and Santillán (2019) are insufficient to explain the dynamic behaviors they observed for the particular set of bacteria chosen for their experiments. Taking this into account, we proposed two alternative model amendments that might account for the reported behaviors: 1) only sensitive and resistant bacteria produce the metabolite sensed by antagonistic bacteria, and 2) all three strains produce metabolite m. However, high population density within the colony triggers metabolic changes in bacterial cells, resulting in little to no participation in several functions like replication, production of metabolite m, or production of the antagonistic substance.

The first alternative represents the most obvious way to solve the problem of bacteria in the periphery of antagonistic colonies responding to other bacteria within the same colony. However, we know beforehand that this model version will not be able to reproduce the observed growth rate decrease of two facing antagonistic colonies. To account for the fact that antagonistic bacteria do not produce metabolite m, the PDE for m is modified as follows:

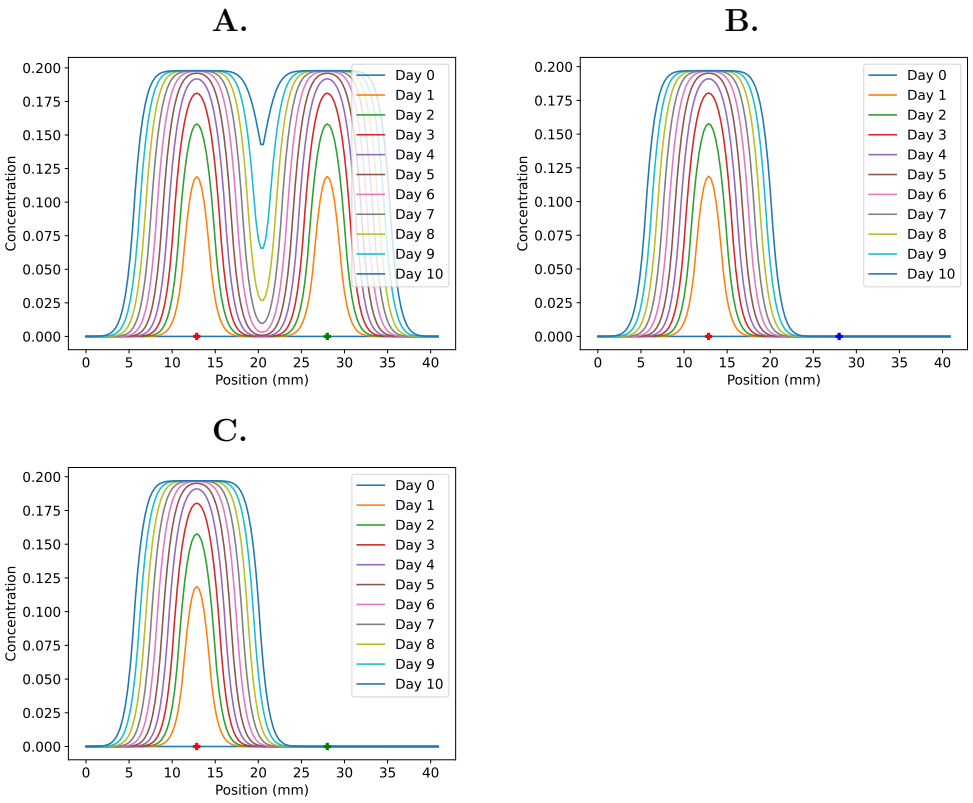

Figure 4.4: Antagonistic substance u profile concentrations for confronted-colonies simulations, A vs A (**A.**), A vs R (**B.**) and A vs S (**C.**). Crosses along the x-axis indicate the center of the colony and the color indicates the strain it belongs to (antagonistic red, resistant blue and sensitive green).

$$\frac{\partial m}{\partial t} = D_m \nabla^2 m + r_m \left(S + R\right) - \gamma_m m. \tag{4.1}$$

While maintaining the same parameter values (see Table 4.1), we simulated the confronted colonies experiments performed by Gallardo-Navarro and Santillán (2019). Results can be observed in Figs. 4.5 to 4.7. Simulations corresponding to two facing antagonistic colonies were not carried out for the above explained reasons.

Figs. 4.5A and B show the differences between external and internal radii for all three strains as a function of time. Our model was able to qualitatively recover the behavior observed by Gallardo-Navarro and Santillán (2019). Notice that in A vs S the effect of substance u over strain S is higher than what it costs A to produce it; however, A vs R shows that the metabolic cost of producing substance u is higher than the cost for R to counteract

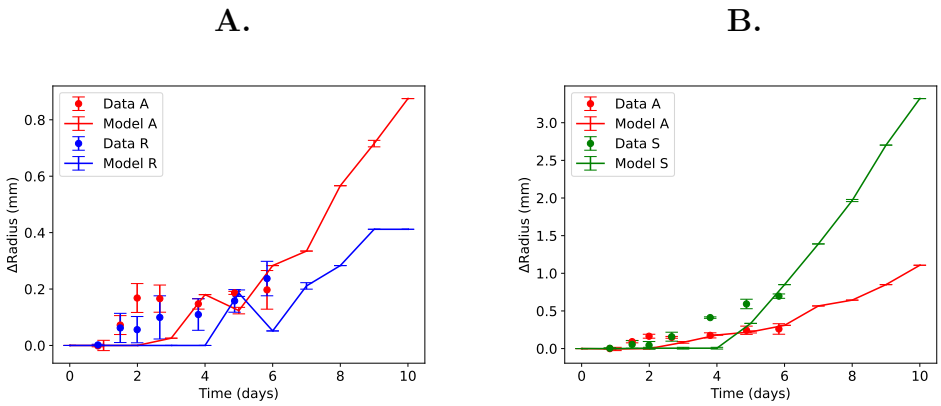

Figure 4.5: Comparison of the simulations of confronted-colonies experiments with the reported experimental results, A vs R (**A.**) and A vs S (**B.**). ΔRadius is defined as the difference between the external and internal radii of the colony. Error bars indicate standard deviation.

it. This last appreciation is not in agreement with experimental observations, where both metabolic costs produced seemingly the same effect.

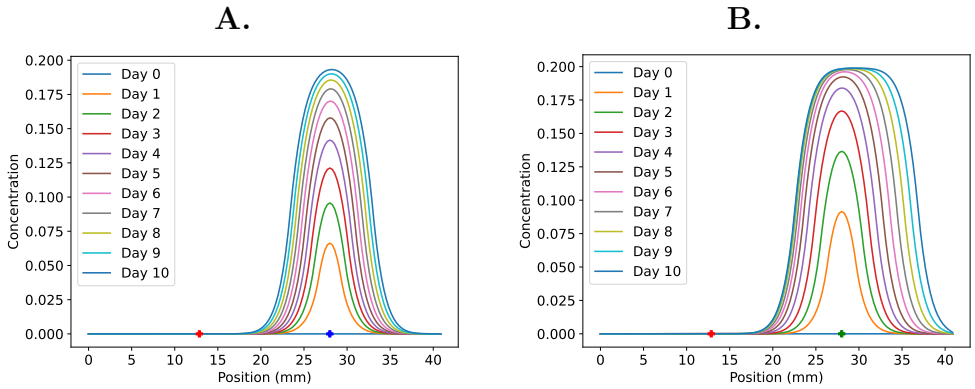

Figure 4.6: Metabolite m profile concentrations for confronted-colonies simulations, A vs R (**A.**) and A vs S (**B.**). Crosses along the x-axis indicate the center of the colony and the color indicates the strain it belongs to (antagonistic red, resistant blue and sensitive green).

Under the new assumption, substance u concentration profiles (Figs. 4.7A and B) show a slightly inclination towards the right, direction in which the sensitive or the resistant colony is located. This happens because it is the presence of metabolite m the responsible for activating the production of substance u, and m is solely secreted by either strain S or R (Figs. 4.6A and B). This proves that unlike in the original model, the mechanism responsible of producing substance u is not active in every bacteria present in the antagonistic colony, but rather in those closer to the source of metabolite m, even when the growth of A is affected by the metabolic cost of producing substance u. Metabolite m concentration profiles on

A vs S are asymmetrical which is evidence of the effect of substance u on the growth of strain S. This is imperceptible in A vs R which we attribute to the resistant strain growing slower than the sensitive strain, and hence it is further apart from the antagonistic colony.

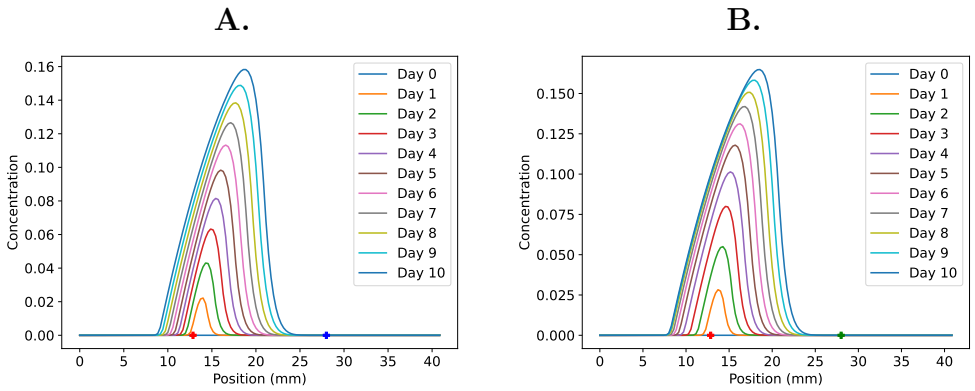

Figure 4.7: Antagonistic substance u profile concentrations for confronted-colonies simulations, A vs R (**A.**) and A vs S (**B.**). Crosses along the x-axis indicate the center of the colony and the color indicates the strain it belongs to (antagonistic red, resistant blue and sensitive green).

Lastly, we simulated artificial bacterial communities experiments performed by Gallardo-Navarro and Santillán (2019) to study local, close range interactions, first between antagonists and sensitive bacteria, followed by a community built with all three strains as described in section 3.6. Gallardo-Navarro and Santillán (2019) reported that antagonistic and sensitive bacteria presented competitive exclusion, whereas resistant and sensitive bacteria, and resistant and antagonistic bacteria presented competitive coexistence. Given that our model is normalized by the corresponding carrying capacity, we took α_{AS}, α_{SA}, α_{RS}, α_{SR}, α_{RA} and α_{AR} (*i.e.* Lotka-Volterra competition parameters) as free parameters, and empirically changed their values provided that $0 < \alpha_{Rj}, \alpha_{iR} < 1.0$ for $i, j = A$ or S and $\alpha_{AS}, \alpha_{SA} > 1.0$, which indicate competitive coexistence and competitive exclusion, respectively. Selected values are listed in Fig. 4.2. The PDE model was solved as described in section 3.6. At the end of the simulated period of time we calculated the area of the simulated mesh occupied by S and plotted it as a function of the initial population of A. The outcomes are presented in Fig. 4.8. Observe that the curve presents a displacement to the right in the presence of resistant bacteria, which means that resistant bacteria aid sensitive bacteria in surviving antagonistic bacteria as reported by Gallardo-Navarro and Santillán (2019). Nonetheless, we were unable to obtain results where either S or A drive the other to extinction, or the more drastic effect of the toxicity of substance u on the well being of sensitive bacteria, which is inconsistent with previous observations (Gallardo-Navarro and Santillán, 2019).

Parameter	Value
α_{AS}	2.0
α_{SA}	1.65
α_{AR}	0.5
α_{RA}	0.6
α_{SR}	0.6
α_{RS}	0.4

Table 4.2: Model parameter values for close-range interactions in artificial communities simulations.

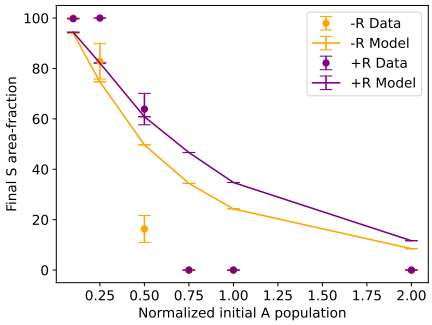

Figure 4.8: Plots of final area-fraction occupied by the sensitive strain as a function of the initial population of antagonistic bacteria in artificial communities. The reported experimental results are represented with points, whereas the simulation results are plotted with solid lines. Orange points/lines correspond to the experiments in which no resistant bacteria are added to the initial mixture, while purple points/lines correspond to the experiments with added resistant bacteria. Error bars indicate standard deviation.

To summarize, assuming that antagonistic bacteria do not produce the metabolite they detect allows the model to qualitatively reproduce many of the experimental results. However, we believe that the outcomes are unsatisfactory, not to mention the model inability to explain antagonistic-bacteria growth-rate decrease in the presence of other antagonistic bacteria. This lead us to analyze a second modification to the original model. Consider that natural selection has established ways of modifying bacteria metabolism to reduce metabolic cost under specific circumstances and when necessary (Stubbendieck et al., 2016; Granato et al., 2019). For example, when bacterial populations reach a high density, bacteria reduce their metabolism and cease participating in processes such as growth, cell division, and metabolite secretion (Horner-Devine et al., 2003; Yeor-Davidi et al., 2020; Bocci et al., 2018; Wolfsberg et al., 2018; Tronnolone et al., 2018; Cole et al., 2015). Instead, they begin to act as a group. This behavior benefits the species by making it less vulnerable, and it is also thought to be the key to antibiotic resistance (Petrof et al., 2013; Yeor-Davidi et al., 2020). To incorporate this into the model, we established all bacteria population above 0.9 as high population density, and fixed their current state. This means that the population stays the same as of that moment, and does not interact in any way with bacteria in adjacent compartments. Aside from this consideration, the PDE model remained the same.

Parameter	A	R	S	m	u
D $(\mathrm{mm}^2/\mathrm{min})$	8.5×10^{-9}	5.1×10^{-9}	8.5×10^{-9}	0.51	0.085
r (min^{-1})	0.0078	0.0047	0.0086	0.2	0.2
K	0.004	3.5×10^{-15}	0.5×10^{-9}	NA	0.8
n	3.0	3.5	3.0	NA	3.5
γ (min^{-1})	NA	NA	NA	0.01	0.01
d	0.45	0.45	NA	NA	NA

Table 4.3: Model parameter values for single-colony and confronted-colonies simulations.

Parameter values estimated for this simulations required additional fine-tuning in order to reproduce Gallardo-Navarro and Santillán (2019) experiments under the new set of assumptions. New parameter values are listed in Table 4.3. We began by simulating the single colony experiments (Fig. 4.9). As with previous assumptions, both antagonistic and sensitive bacteria show a higher differential coefficient than resistant bacteria, consistent with previous observations (Gallardo-Navarro and Santillán, 2019). Notice that once again, our model can only qualitatively emulate the experimental growth curves, since no amendments were made in this regard.

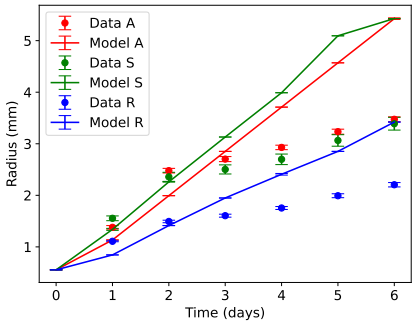

Figure 4.9: Comparison of the simulations of single colonies growing on agar (solid lines) and the corresponding reported experimental results (points). Error bars indicate standard deviation.

We then simulated the neighboring colony experiments by solving the PDE system as described in section 3.2. The outcomes are contrasted in Figs. 4.10 to 4.12 with experimental data. As shown in Figs. 4.10A-C, the model is capable of qualitatively reproducing the

experimentally observed behavior in all three situations. That is, all three bacterial strains grow at a slower rate when faced with an antagonistic colony. In spite of this, our model could not induce an early response in any of the bacterial strains as opposed to the previously described models or the experimental data (Gallardo-Navarro and Santillán, 2019). Observe that we only recorded data for 7 simulated days when facing an antagonistic with a sensitive colony, this due to the fact that after 7 simulated days, the sensitive colony had outgrown the mesh and we could no longer measure the external radius.

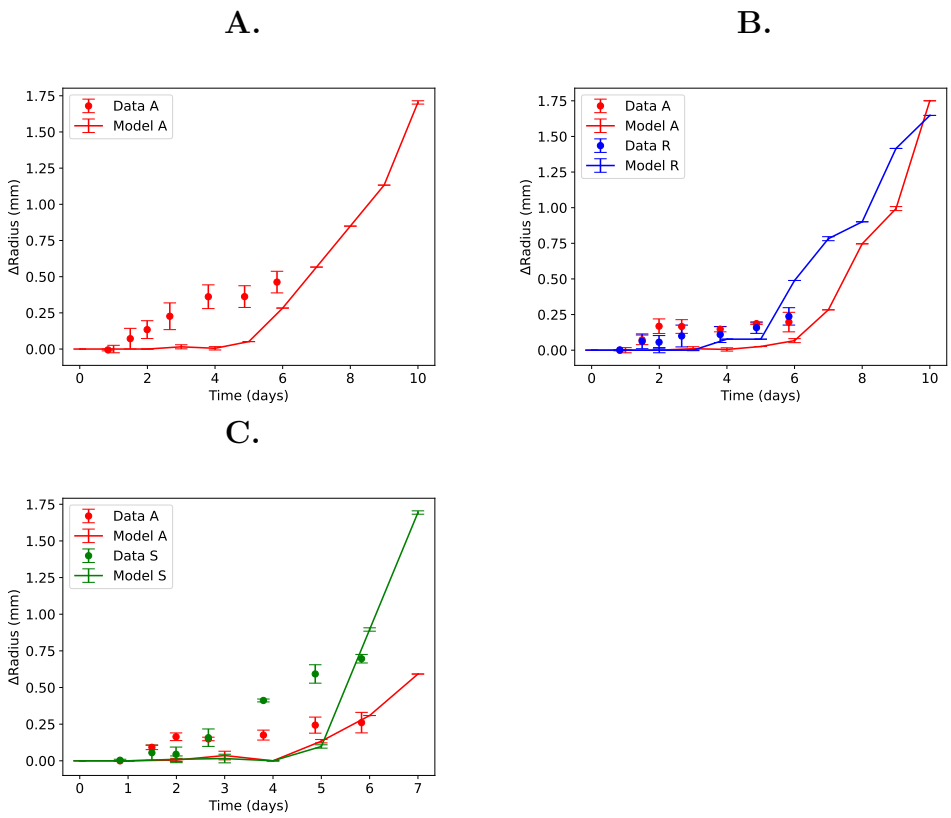

Figure 4.10: Comparison of the simulations of confronted-colonies experiments with the reported experimental results, A vs A (**A.**), A vs R (**B.**) and A vs S (**C.**). ΔRadius is defined as the difference between the external and internal radii of the colony. Error bars indicate standard deviation.

Metabolite profiles (Figs. 4.11A-C) show a higher accumulation of metabolite m between the two colonies than in any other place, which translates in an increased production of substance u in the direction of the facing colony as observed in substance u profiles (Figs. 4.12A-C) and also accounts for the concomitant metabolic cost evidenced in Fig. 4.10A. As in the first amended model, there is not a generalized production of antagonistic substance, and it is only produced among bacteria located where there is higher accumulation of metabolite m.

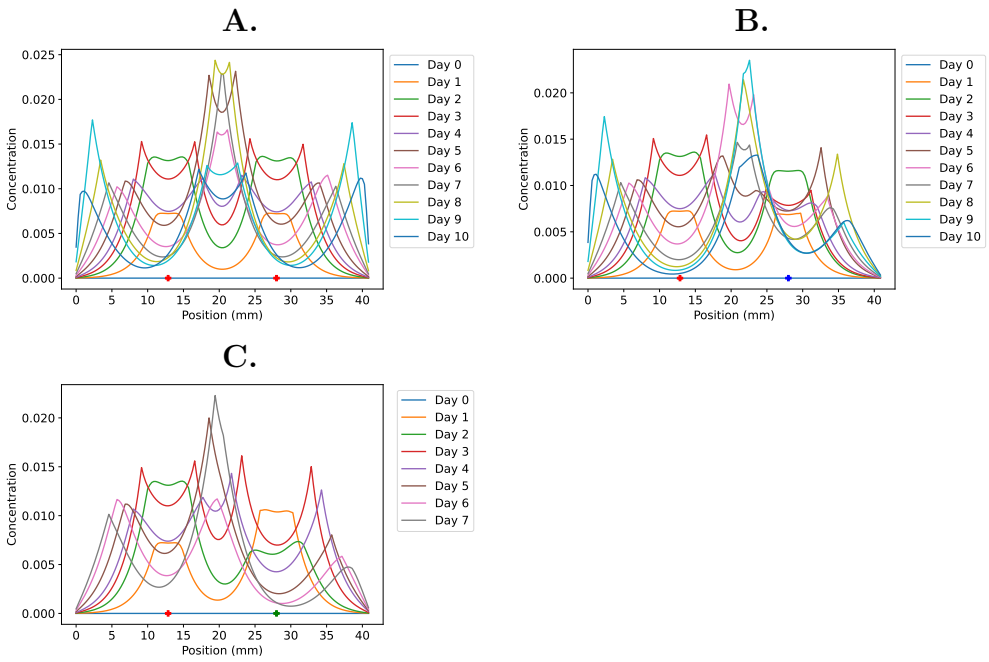

Figure 4.11: Metabolite m profile concentrations for confronted-colonies simulations, A vs A (**A.**), A vs R (**B.**) and A vs S (**C.**). Crosses along the x-axis indicate the center of the colony and the color indicates the strain it belongs to (antagonistic red, resistant blue and sensitive green).

We also simulated the artificial bacterial communities experiments performed by Gallardo-Navarro and Santillán (2019). Data was recorded for 10 simulated days in communities without resistant bacteria, and for 14 simulated days in communities with resistant bacteria as in both cases, the system had already reached a steady state (not shown). Results are plotted in Fig. 4.13 and the re-estimated values for parameters indicating close range competition (α_{ij} with $i, j = A, S$ or R) are listed in Table 4.4. Observe that the model qualitatively recovers the reported behavior (Gallardo-Navarro and Santillán, 2019). In the presence of resistant bacteria there is a displacement of the curve to the right, which indicates that resistant bacteria aid sensitive bacteria to survive in the presence of antagonists. Unlike what was observed in the previous scenario, it is possible to recreate the situations where either antagonists or sensitive bacteria drive the other to extinction.

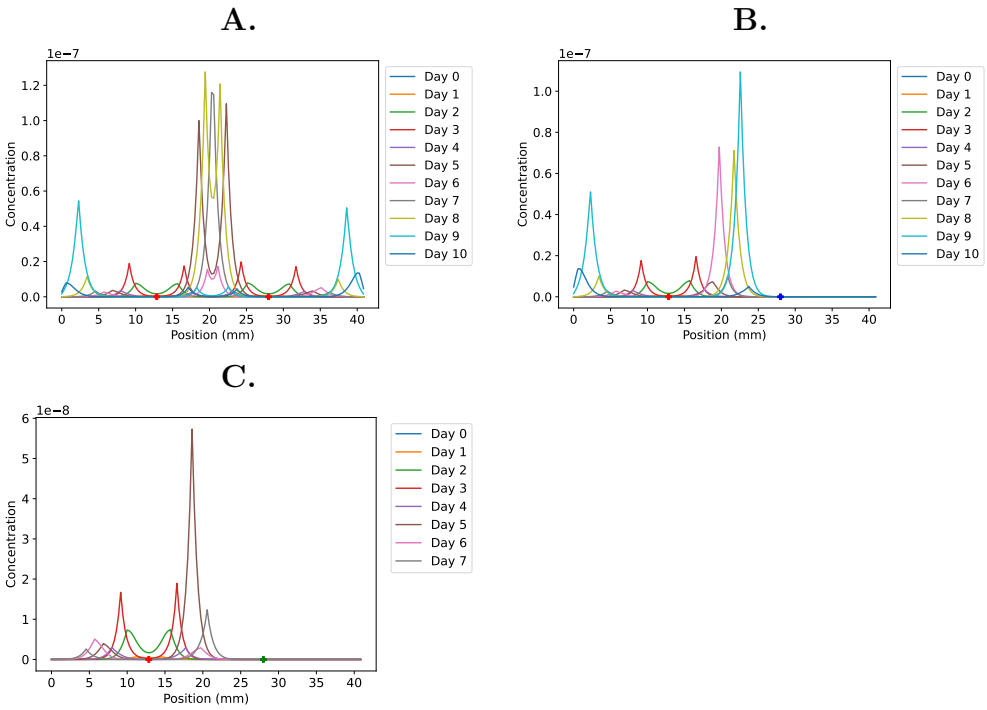

Figure 4.12: Antagonistic substance u profile concentrations for confronted-colonies simulations, A vs A (**A.**), A vs R (**B.**) and A vs S (**C.**). Crosses along the x-axis indicate the center of the colony and the color indicates the strain it belongs to (antagonistic red, resistant blue and sensitive green).

Parameter	Value
α_{AS}	2.0
α_{SA}	1.7
α_{AR}	0.37
α_{RA}	0.65
α_{SR}	0.44
α_{RS}	0.65

Table 4.4: Model parameter values for close-range interactions in artificial communities simulations.

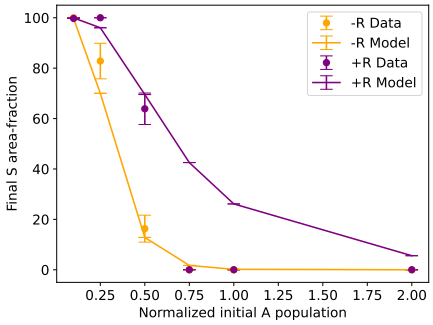

Figure 4.13: Plots of final area-fraction occupied by the sensitive strain as a function of the initial population of antagonistic bacteria in artificial communities. The reported experimental results are represented with points, whereas the simulation results are plotted with solid lines. Orange points/lines correspond to the experiments in which no resistant bacteria are added to the initial mixture, while purple points/lines correspond to the experiments with added resistant bacteria. Error bars indicate standard deviation.

Chapter 5

Concluding Remarks

We studied the dynamics of competition and antagonistic interactions mediated by diffusive agents of an artificial community of bacteria growing on solid medium. The purpose of this project was to determine whether a specific antagonism mechanisms could explain how resistant bacteria increase the likelihood of survival of sensitive bacteria when in a community with antagonistic bacteria (Gallardo-Navarro and Santillán, 2019).

We developed a mathematical model describing a community of three bacterial strains: a sensitive, a resistant, and an antagonistic strain to explore the antagonism mechanisms proposed by Gallardo-Navarro and Santillán (2019). Antagonistic bacteria detect the proximity of other bacteria by sensing an increase in the concentration of a common metabolite that diffuses in the medium. In response, antagonistic bacteria produce an antagonistic substance, albeit at a metabolic cost. Said antagonistic substance kills and impedes the growth of sensitive bacteria. By incurring a metabolic cost, resistant bacteria are able to counteract the effects of the antagonistic substance. Moreover, the presence of resistant bacteria limits the growth of antagonistic bacteria, benefiting sensitive bacteria.

Our results suggested that although the mechanisms proposed by Gallardo-Navarro and Santillán (2019) are able to explain the toxic effect of the antagonistic substance over the growth and well being of sensitive bacteria, and the metabolic cost resistant bacteria have to pay in order to counteract the toxicity, they are insufficient to reproduce the metabolic cost of producing the antagonistic substance. In this regard we proposed two alternative model amendments:

1. Only sensitive and resistant bacteria produce the metabolite.

2. Due to high population density within the colony, bacteria undergo metabolic changes

and no longer participate in functions such as replication, migration and metabolite or antagonistic substance production.

The first alternative could explain the majority of the experimental results from Gallardo-Navarro and Santillán (2019), but it was insufficient as well because it could not reproduce the concomitant metabolic cost of producing the antagonistic substance. The second alternative provided a better explanation to the behavior observed by Gallardo-Navarro and Santillán (2019). Based on these findings, we hypothesize that the mechanisms described above can explain how the presence of resistant bacteria may help sensitive bacteria survive, but only when bacteria undergo significant phenotypic changes at high population densities. Note that the current study considers 2-dimensional bacterial communities growing on a solid substrate, which limits the validity of the previous conclusion to bacterial communities growing under similar conditions.

Resistant bacteria increasing the likelihood of survival of sensitive bacteria in the presence of antagonistic bacteria is not unheard of Aguilar-salinas and Olmedo-álvarez (2022); Iven et al. (2023). The mechanisms responsible have not been clearly identified, but horizontal gene transfer appears to be at the root of several such observations. Interestingly, the current study supports the existence of a different non-genetic mechanism that achieves a similar result (at least for bacteria growing on solid substrate), and emphasizes the importance of spatial distribution on microbial population dynamics. Our results along with previously reported observations suggest that bacteria have developed more than one mechanism that grants sensitive bacteria the possibility of surviving in complex communities, despite the various antagonistic interactions surrounding them, a phenomenon denominated facilitation (Iven et al., 2023). It is worth mentioning that the mechanisms here proposed are just one of many attempts of understanding what underlies biodiversity in bacterial communities and could be use as a tool to suggest future experimental studies.

Chapter 6

Perspectives

In this project we were interested in studying facilitation (the phenomenon by which a bacterial strain aids another to survive in the presence of antagonism) among a small artificial community of bacteria as an indirect result of purely antagonistic interactions via a mathematical model. Our findings suggest that this is possible as long as bacteria undergo significant metabolic changes. Determining whether the emerging properties we observed are general enough to arise in conditions different than those explored in this project would be the next step. In this regard we propose two different approaches using mathematical modeling. On the one hand, increasing the size of the community while maintaining the two-dimensional condition. Here, we used an artificial community of three bacterial strains (an antagonistic, a sensitive and a resistant strain), however, bacterial communities are biodiverse, hence establishing if the mechanisms discussed in this work produce comparable behaviors as those observed experimentally would provide insight in a perspective different than horizontal gene transfer. On the other hand, studying the same community in a three-dimensional space. Considering a third dimension where bacterial aggregates and metabolite diffusion behaves differently than in two-dimensions, and therefore exploring if the antagonistic mechanisms we proposed are robust enough to hold at least theoretically, could be used as a tool to suggest experimental projects as well.

References

B. Aguilar-salinas and G. Olmedo-álvarez. A three-strain synthetic community model whose rapid response to antagonism allows the study of higher-order dynamics and emergent properties in minutes. 2022.

E. Aguirre-von Wobeser, L. E. Eguiarte, V. Souza, and G. Soberón-Chávez. Theoretical analysis of the cost of antagonistic activity for aquatic bacteria in oligotrophic environments. *Frontiers in Microbiology*, 6(MAY):1–8, 2015. ISSN 1664302X. doi: 10.3389/fmicb.2015.00490.

T. Ahmed, T. S. Shimizu, and R. Stocker. Bacterial chemotaxis in linear and nonlinear steady microfluidic gradients. *Nano Letters*, 10(9):3379–3385, 2010. ISSN 15306984. doi: 10.1021/nl101204e.

C. A. Biggs, O. I. Olaleye, L. F. Jeanmeure, P. Deines, H. S. Jensen, S. J. Tait, and P. C. Wright. Effect of temperature on the substrate utilization profiles of microbial communities in different sewer sediments. *Environmental Technology*, 32(2):133–144, 2011. ISSN 1479487X. doi: 10.1080/09593330.2010.490852.

A. E. Blanchard and T. Lu. Bacterial social interactions drive the emergence of differential spatial colony structures. *BMC Systems Biology*, 59(9):1–13, 2015. ISSN 17520509. doi: 10.1186/s12918-015-0188-5.

F. Bocci, Y. Suzuki, M. Lu, and J. N. Onuchic. Role of metabolic spatiotemporal dynamics in regulating biofilm colony expansion. *Proceedings of the National Academy of Sciences of the United States of America*, 115(16):4288–4293, 2018. ISSN 10916490. doi: 10.1073/pnas.1706920115.

I. M. Bomze. Lotka-Volterra equation and replicator dynamics: A two-dimensional classification. *Biological Cybernetics*, 48:201–211, 1983.

R. Cerritos, L. E. Eguiarte, M. Avitia, J. Siefert, M. Travisano, A. Rodríguez-Verdugo, and V. Souza. Diversity of culturable thermo-resistant aquatic bacteria along an environmental

gradient in Cuatro Ciénegas, Coahuila, México. *Springer*, 99(2):303–318, 2010. ISSN 00036072. doi: 10.1007/s10482-010-9490-9.

S. Y. Cheng, S. Heilman, M. Wasserman, S. Archer, M. L. Shuler, and M. Wu. A hydrogel-based microfluidic device for the studies of directed cell migration. *Lab on a Chip*, 7(6): 763–769, 2007. ISSN 14730189. doi: 10.1039/b618463d.

J. A. Cole, L. Kohler, J. Hedhli, and Z. Luthey-Schulten. Spatially-resolved metabolic cooperativity within dense bacterial colonies. *BMC Systems Biology*, 9(1):1–17, 2015. ISSN 17520509. doi: 10.1186/s12918-015-0155-1.

O. X. Cordero and M. S. Datta. Microbial interactions and community assembly at microscales. *Current Opinion in Microbiology*, 31(Figure 1):227–234, 2016. ISSN 18790364. doi: 10.1016/j.mib.2016.03.015.

C. R. Currie. A community of ants, fungi, and bacteria: A multilateral approach to studying symbiosis. *Annual Review of Microbiology*, 55:357–380, 2001. ISSN 00664227. doi: 10.1146/annurev.micro.55.1.357.

T. L. Czárán, R. F. Hoekstra, and L. Pagie. Chemical warfare between microbes promotes biodiversity. *Pnas*, 99(2):786–790, 2002.

R. Daniels, J. Vanderleyden, and J. Michiels. Quorum sensing and swarming migration in bacteria. *FEMS Microbiology Reviews*, 28(3):261–289, 2004. ISSN 01686445. doi: 10.1016/j.femsre.2003.09.004.

J. De Vrieze, M. E. Christiaens, and W. Verstraete. The microbiome as engineering tool: Manufacturing and trading between microorganisms. *New Biotechnology*, 39:206–214, 2017. ISSN 18764347. doi: 10.1016/j.nbt.2017.07.001. URL `https://doi.org/10.1016/j.nbt.2017.07.001`.

E. F. DeLong and N. R. Pace. Environmental diversity of bacteria and archaea. *Systematic Biology*, 50(4):470–478, 2001. ISSN 10635157. doi: 10.1080/106351501750435040.

J. Diao, L. Young, S. Kim, E. A. Fogarty, S. M. Heilman, P. Zhou, M. L. Shuler, M. Wu, and M. P. DeLisa. A three-channel microfluidic device for generating static linear gradients and its application to the quantitative analysis of bacterial chemotaxis. *Lab on a Chip*, 6 (3):381–388, 2006. ISSN 14730189. doi: 10.1039/b511958h.

M. D. Dressler, J. Conde, O. T. Eldakar, and R. P. Smith. Timing between successive introduction events determines establishment success in bacteria with an Allee effect. *Proceedings of the Royal Society B: Biological Sciences*, 286(1902), 2019. ISSN 14712954. doi: 10.1098/rspb.2019.0598.

P. G. Falkowski, T. Fenchel, and E. F. Delong. The microbial engines that drive earth's biogeochemical cycles. *Science*, 320(5879):1034–1039, 2008. ISSN 00368075. doi: 10.1126/science.1153213.

M. Frean and E. R. Abraham. Rock–scissors–paper and the survival of the weakest. *Proceedings of the Royal Society of London. Series B: Biological Sciences*, 268(1474):1323–1327, jul 2001. ISSN 0962-8452. doi: 10.1098/rspb.2001.1670.

J. Friedman and J. Gore. Ecological systems biology: The dynamics of interacting populations. *Current Opinion in Systems Biology*, 1:114–121, 2017. ISSN 24523100. doi: 10.1016/j.coisb.2016.12.001.

Ó. A. Gallardo-Navarro and M. Santillán. Three-way interactions in an artificial community of bacterial strains directly isolated from the environment and their effect on the system population dynamics. *Frontiers in Microbiology*, pages 1–13, 2019.

S. J. Giovannoni and K. L. Vergin. Seasonality in ocean microbial communities. *Science*, 335 (6069):671–676, 2012. ISSN 10959203. doi: 10.1126/science.1198078.

M. Goswami, P. Bhattacharyya, and P. Tribedi. Allee effect: the story behind the stabilization or extinction of microbial ecosystem. *Archives of Microbiology*, 199(2):185–190, 2017. ISSN 1432072X. doi: 10.1007/s00203-016-1323-4.

E. T. Granato, T. A. Meiller-Legrand, and K. R. Foster. The Evolution and Ecology of Bacterial Warfare. *Current Biology*, 29(11):R521–R537, jun 2019. ISSN 09609822. doi: 10.1016/j.cub.2019.04.024.

E. K. Hall, C. Neuhauser, and J. B. Cotner. Toward a mechanistic understanding of how natural bacterial communities respond to changes in temperature in aquatic ecosystems. *ISME Journal*, 2(5):471–481, 2008. ISSN 17517362. doi: 10.1038/ismej.2008.9.

R. M. Harshey. Bees aren't the only ones: swarming in Gram-negative bacteria. *Molecular Microbiology*, 13(3):389–394, 1994. ISSN 13652958. doi: 10.1111/j.1365-2958.1994.tb00433.x.

R. M. Harshey. Bacterial Motility on a Surface: Many Ways to a Common Goal. *Annual Review of Microbiology*, 57:249–273, 2003. ISSN 00664227. doi: 10.1146/annurev.micro.57.030502.091014.

F. J. Hol, P. Galajda, R. G. Woolthuis, C. Dekker, and J. E. Keymer. The idiosyncrasy of spatial structure in bacterial competition. *BMC Research Notes*, 245(8):1–7, 2015. ISSN 17560500. doi: 10.1186/s13104-015-1169-x.

M. C. Horner-Devine, K. M. Carney, and B. J. Bohannan. An ecological perspective on bacterial biodiversity. *Proceedings of the Royal Society B: Biological Sciences*, 271(1535): 113–122, 2003. ISSN 14712970. doi: 10.1098/rspb.2003.2549.

H. Iven, T. W. Walker, and M. Anthony. Biotic Interactions in Soil are Underestimated Drivers of Microbial Carbon Use Efficiency. *Current Microbiology*, 80(1):1–14, 2023. ISSN 14320991. doi: 10.1007/s00284-022-02979-2. URL `https://doi.org/10.1007/s00284-022-02979-2`.

S. Jeanson, J. Floury, V. Gagnaire, S. Lortal, and A. Thierry. Bacterial Colonies in Solid Media and Foods: A Review on Their Growth and Interactions with the Micro-Environment. *Frontiers in Microbiology*, 6(December), dec 2015. ISSN 1664-302X. doi: 10.3389/fmicb.2015.01284.

R. B. Kaul, A. M. Kramer, F. C. Dobbs, and J. M. Drake. Experimental demonstration of an Allee effect in microbial populations. *Biology Letters*, 12(4), 2016. ISSN 1744957X. doi: 10.1098/rsbl.2016.0070.

M. J. Kennedy and P. A. Volz. Ecology of Candida albicans gut colonization: Inhibition of Candida adhesion, colonization, and dissemination from the gastrointestinal tract by bacterial antagonism. *Infection and Immunity*, 49(3):654–663, 1985. ISSN 00199567. doi: 10.1128/iai.49.3.654-663.1985.

B. Kerr, M. A. Riley, M. W. Feldman, and B. J. Bohannan. Local dispersal promotes biodiversity in a real-life game of rock-paper-scissors. *Nature*, 418(6894):171–174, 2002. ISSN 00280836. doi: 10.1038/nature00823.

B. H. Kim and G. M. Gadd. *Bacterial physiology and metabolism*. Cambridge, 2008. ISBN 9780521846363.

W. Kim, K. Hwang, S. G. Shin, S. Lee, and S. Hwang. Effect of high temperature on bacterial community dynamics in anaerobic acidogenesis using mesophilic sludge inoculum.

Bioresource Technology, 101(SUPPL.1):S17–S22, 2010. ISSN 09608524. doi: 10.1016/j.biortech.2009.03.029. URL http://dx.doi.org/10.1016/j.biortech.2009.03.029.

B. C. Kirkup and M. A. Riley. Antibiotic-mediated antagonism leads to a bacterial game of rock-paper-scissors in vivo. *Nature*, 428(6981):412–414, 2004. ISSN 00280836. doi: 10.1038/nature02429.

M. L. Knope, A. M. Bush, L. O. Frishkoff, N. A. Heim, and J. L. Payne. Ecologically diverse clades dominate the oceans via extinction resistance. *Science*, 1038(February):in press, 2020.

A. Koeppel, E. B. Perry, J. Sikorski, D. Krizanc, A. Warner, D. M. Ward, A. P. Rooney, E. Brambilla, N. Connor, R. M. Ratcliff, E. Nevo, and F. M. Cohan. Identifying the fundamental units of bacterial diversity: A paradigm shift to incorporate ecology into bacterial systematics. *Proceedings of the National Academy of Sciences of the United States of America*, 105(7):2504–2509, 2008. ISSN 00278424. doi: 10.1073/pnas.0712205105.

R. J. LeVeque. *Finite Difference Methods for Ordinary and Partial Differential Equations*. Society for Industrial and Applied Mathematics, 2007. ISBN 9780898716290. doi: https://doi.org/10.1137/1.9780898717839.

A. D. Martins and E. Gjini. Modeling Competitive Mixtures With the Lotka-Volterra Framework for More Complex Fitness Assessment Between Strains. *Frontiers in Microbiology*, 11(September):1–11, 2020. doi: 10.3389/fmicb.2020.572487.

M. Matsushita, J. Wakita, H. Itoh, K. Watanabe, T. Arai, T. Matsuyama, H. Sakaguchi, and M. Mimura. Formation of colony patterns by a bacterial cell population. *Physica A: Statistical Mechanics and its Applications*, 274(1):190–199, 1999. ISSN 03784371. doi: 10.1016/S0378-4371(99)00328-3.

L. L. McCarter. Dual flagellar systems enable motility under different circumstances. *Journal of Molecular Microbiology and Biotechnology*, 7(1-2):18–29, 2004. ISSN 14641801. doi: 10.1159/000077866.

M. Mimura, H. Sakaguchi, and M. Matsushita. Reaction-diffusion modelling of bacterial colony patterns. *Physica A: Statistical Mechanics and its Applications*, 282(1):283–303, 2000. ISSN 03784371. doi: 10.1016/S0378-4371(00)00085-6.

M. A. O'Malley. The nineteenth century roots of 'everything is everywhere'. *Nature Reviews Microbiology*, 5(8):647–651, 2007. ISSN 17401526. doi: 10.1038/nrmicro1711.

L. Oña and C. Kost. Cooperation increases robustness to ecological disturbance in microbial cross-feeding networks. *Ecology Letters*, (August 2021):1–11, 2022. ISSN 1461-023X. doi: 10.1111/ele.14006.

A. R. Pacheco and D. Segrè. A multidimensional perspective on microbial interactions. *FEMS Microbiology Letters*, 366(11):1–11, 2019. ISSN 15746968. doi: 10.1093/femsle/fnz125.

R.-A. Pérez-Gutiérrez, V. López-Ramírez, Á. Islas, L. D. Alcaraz, I. Hernández-González, B. C. L. Olivera, M. Santillán, L. E. Eguiarte, V. Souza, M. Travisano, and G. Olmedo-Alvarez. Antagonism influences assembly of a Bacillus guild in a local community and is depicted as a food-chain network. *The ISME Journal*, 7(3):487–497, mar 2013. ISSN 1751-7362. doi: 10.1038/ismej.2012.119.

E. O. Petrof, G. B. Gloor, S. J. Vanner, S. J. Weese, D. Carter, M. C. Daigneault, E. M. Brown, K. Schroeter, and E. Allen-Vercoe. Stool substitute transplant therapy for the eradication of Clostridium difficile infection: 'RePOOPulating' the gut. *Microbiome*, 1(1): 1–12, 2013. ISSN 20492618. doi: 10.1186/2049-2618-1-3.

L. Z. Pipe and M. J. Grimson. Spatial-temporal modelling of bacterial colony growth on solid media. *Molecular BioSystems*, 4(3):192, 2008. ISSN 1742-206X. doi: 10.1039/b708241j.

M. A. Pires, N. Crokidakis, and S. M. Duarte Queirós. Randomness in ecology: The role of complexity on the Allee effect. *Physica A: Statistical Mechanics and its Applications*, 589:126548, 2022. ISSN 03784371. doi: 10.1016/j.physa.2021.126548. URL `https://doi.org/10.1016/j.physa.2021.126548`.

J. J. Qian and E. Akçay. The balance of interaction types determines the assembly and stability of ecological communities. *Nature Ecology and Evolution*, 4(3):356–365, mar 2020. ISSN 2397-334X. doi: 10.1038/s41559-020-1121-x.

N. S. N. A. Rahman, N. W. A. Hamid, and K. Nadarajah. Effects of abiotic stress on soil microbiome. *International Journal of Molecular Sciences*, 22(16), 2021. ISSN 14220067. doi: 10.3390/ijms22169036.

C. Ratzke, J. Barrere, and J. Gore. Strength of species interactions determines biodiversity and stability in microbial communities. *Nature Ecology and Evolution*, 4(3):376–383, 2020. ISSN 2397334X. doi: 10.1038/s41559-020-1099-4.

T. Reichenbach, M. Mobilia, and E. Frey. Mobility promotes and jeopardizes biodiversity in rock-paper-scissors games. *Nature*, 448(7157):1046–1049, 2007. ISSN 14764687. doi: 10.1038/nature06095.

A. Retter, C. Karwautz, and C. Griebler. Groundwater microbial communities in times of climate change. *Current Issues in Molecular Biology*, 41:509–538, 2021. ISSN 14673045. doi: 10.21775/cimb.041.509.

C. L. Richards, Y. Hanzawa, M. S. Katari, I. M. Ehrenreich, K. E. Engelmann, and M. D. Purugganan. Perspectives on Ecological and Evolutionary Systems Biology. *Annual Plant Reviews online*, 35:331–349, 2018. doi: 10.1002/9781119312994.apr0383.

R. Smith, C. Tan, J. K. Srimani, A. Pai, K. A. Riccione, H. Song, and L. You. Programmed Allee effect in bacteria causes a tradeoff between population spread and survival. *Proceedings of the National Academy of Sciences of the United States of America*, 111(5): 1969–1974, 2014. ISSN 00278424. doi: 10.1073/pnas.1315954111.

R. M. Stubbendieck and P. D. Straight. Multifaceted interfaces of bacterial competition. *Journal of Bacteriology*, 198(16):2145–2155, 2016. ISSN 10985530. doi: 10.1128/JB.00275-16.

R. M. Stubbendieck, C. Vargas-Bautista, and P. D. Straight. Bacterial communities: Interactions to scale. *Frontiers in Microbiology*, 7:1–19, 2016. ISSN 1664302X. doi: 10.3389/fmicb.2016.01234.

E. W. Tekwa, D. Nguyen, D. Juncker, M. Loreau, and A. Gonzalez. Patchiness in a microhabitat chip affects evolutionary dynamics of bacterial cooperation. *Lab on a Chip*, 15(18): 3723–3729, 2015. ISSN 14730189. doi: 10.1039/c5lc00576k.

R. P. Tittsler and L. A. Sandholzer. The Use of Semi-solid Agar for the Detection of Bacterial Motility. *Journal of bacteriology*, 31(6):575–80, 1936. ISSN 0021-9193.

H. Tronnolone, A. Tam, Z. Szenczi, J. E. Green, S. Balasuriya, E. L. Tek, J. M. Gardner, J. F. Sundstrom, V. Jiranek, S. G. Oliver, and B. J. Binder. Diffusion-Limited Growth of Microbial Colonies. *Scientific Reports*, 8(1):1–11, 2018. ISSN 20452322. doi: 10.1038/s41598-018-23649-z.

P. J. Turnbaugh, R. E. Ley, M. Hamady, C. M. Fraser-Liggett, R. Knight, and J. I. Gordon. The Human Microbiome Project. *Nature*, 449(7164):804–810, 2007. ISSN 14764687. doi: 10.1038/nature06244.

O. S. Venturelli, A. V. Carr, G. Fisher, R. H. Hsu, R. Lau, B. P. Bowen, S. Hromada, T. Northen, and A. P. Arkin. Deciphering microbial interactions in synthetic human gut microbiome communities. *Molecular Systems Biology*, 14(6):1–19, 2018. ISSN 1744-4292. doi: 10.15252/msb.20178157.

E. Wolfsberg, C. P. Long, and M. R. Antoniewicz. Metabolism in dense microbial colonies: 13 C metabolic flux analysis of E. coli grown on agar identifies two distinct cell populations with acetate cross-feeding. *Metabolic Engineering*, 49(August):242–247, 2018. ISSN 10967184. doi: 10.1016/j.ymben.2018.08.013. URL `https://doi.org/10.1016/j.ymben.2018.08.013`.

E. Yeor-Davidi, M. Zverzhinetsky, V. Krivitsky, and F. Patolsky. Real-time monitoring of bacterial biofilms metabolic activity by a redox-reactive nanosensors array. *Journal of Nanobiotechnology*, 18(1):1–11, 2020. ISSN 14773155. doi: 10.1186/s12951-020-00637-y. URL `https://doi.org/10.1186/s12951-020-00637-y`.

R. Zapién-Campos, G. Olmedo-Álvarez, and M. Santillán. Antagonistic interactions are sufficient to explain self-assemblage of bacterial communities in a homogeneous environment: a computational modeling approach. *Frontiers in Microbiology*, 6(MAY):1–9, may 2015. ISSN 1664-302X. doi: 10.3389/fmicb.2015.00489.

M.-P. Zorzano, D. Hochberg, M.-T. Cuevas, and J.-M. Gómez-Gómez. Reaction-diffusion model for pattern formation in E. coli swarming colonies with slime. *Physical Review E*, 71(3), mar 2005. doi: 10.1103/physreve.71.031908. URL `https://doi.org/10.1103{%}2Fphysreve.71.031908`.

M. H. Zwietering, I. Jongenburger, F. M. Rombouts, and K. Van't Riet. Modeling of the bacterial growth curve. *Applied and Environmental Microbiology*, 56(6):1875–1881, 1990. ISSN 00992240. doi: 10.1128/aem.56.6.1875-1881.1990.